We are IntechOpen, the world's leading publisher of Open Access books Built by scientists, for scientists

4,800
Open access books available

122,000
International authors and editors

135M
Downloads

Our authors are among the

154
Countries delivered to

TOP 1%
most cited scientists

12.2%
Contributors from top 500 universities

CLARIVATE ANALYTICS BOOK CITATION INDEX INDEXED

WEB OF SCIENCE™

Selection of our books indexed in the Book Citation Index in Web of Science™ Core Collection (BKCI)

Interested in publishing with us?
Contact book.department@intechopen.com

Numbers displayed above are based on latest data collected.
For more information visit www.intechopen.com

Chapter

Ferroelectric Polymer PVDF-Based Nanogenerator

Jeongjae Ryu, Seongmun Eom, Panpan Li, Chi Hao Liow and Seungbum Hong

Abstract

This chapter deals with the development of ferroelectric polymer polyvinylidene fluoride (PVDF)-based nanogenerators. Due to its inherent flexibility, PVDF has been studied for application in nanogenerators. We first introduce PVDF and its copolymers, and briefly discuss their properties. Then, we discuss fabrication methods, including solution casting, spin coating, template-assisted method, electrospinning, thermal drawing, and dip coating. Using these methods, a wide variety of ferroelectric polymer structures can be fabricated. In addition to the performance enhancements provided by fabrication methods, the performance of PVDF-based nanogenerators has been improved by incorporating fillers that can alter the factors affecting the performance. Next, we review energy sources that can be exploited by PVDF-based nanogenerators to harvest electricity. The abundant energy sources in the environment include sound, wind flow, and thermal fluctuation. Finally, we discuss implantable PVDF-based nanogenerators. Another advantage of PVDF is its biocompatibility, which enables implantable nanogenerators. We believe that this chapter can also be helpful to researchers who study sensors and actuators as well as nanogenerators.

Keywords: PVDF, nanogenerator, biocompatibility, flexibility, ferroelectric material

1. Introduction

All electronic devices need electrical energy to operate. Although fossil fuels have been the primary sources of that electrical energy to date, alternatives are emerging. This is particularly important given the ongoing proliferation of portable devices. For example, as "big data" has become increasingly important for monitoring structures, healthcare services, smart cites, and so on, there has been an explosion of sensors to collect that information [1–3]. These sensors can even be located in the human body, beneath the human skin, and inside personal wearable devices [4–7]. In such cases, batteries cannot be easily charged or repeatedly replaced. To meet the energy requirements of remote or inaccessible application like these, one of the most promising alternatives to conventional batteries is a nanogenerator, which can convert mechanical energy or thermal fluctuations in the ambient environment into electricity.

Polyvinylidene fluoride (PVDF) and its copolymers, ferroelectric polymers, are ideal candidates for use in nanogenerators. Their unique properties include their high flexibility, lightness, chemical stability, and relatively simple manufacturing

Materials	Microstructures	Structures	Open-circuit voltage	Short-circuit current	Power	References
P(VDF-TrFE)	—	Flat film	7 V	58 nA	—	[12]
P(VDF-TrFE)	—	Curved film	120 V	700 μA	3.9 $mW{\cdot}cm^{-2}$	[13]
PVDF	—	Fabric	14 V @ 0.1 MPa	29.8 μA @ 0.1 MPa	5.1 $\mu W{\cdot}m^{-2}$	[14]
PVDF/$Ba(Ti_{0.9}Zr_{0.1})O_3$	Nanocubes	Flat film	11.99 V @ 11 N	1.36 μA @ 11 N		[15]
PVDF/SnO_2	Nanosheets	Flat film	42 V	6.25 $\mu A{\cdot}cm^{-2}$	4900 $W{\cdot}m^{-3}$	[16]
PVDF/ZnO	Nanoparticles	Flat film	24.5 V @ 28 N	1.7 μA @ 28 N		[17]
PVDF/ZnO	Nanowires	Flat film	6.9 V	0.96 μA	6.624 μW	[18]
PVDF/AlO-rGO	Nanoparticles	Flat film	36 V @ 31.19 kPa	0.8 μA @ 31.19 kPa	27.97 μW	[19]
PVDF/$BaTiO_3$	Nanoparticles	Flat film	10 $V_{peak\text{-}peak}$ @ 2 N	2.5 $\mu A_{peak\text{-}peak}$ @ 2 N	5.8 μW	[20]
PVDF/$BaTiO_3$	Nanowires	Flat film	14 V	4 μA	1.5 μW	[21]
PVDF/NKNS-LT-BZ	Nanoparticles	Flat film	18 V @ 50 N	2.6 μA @ 50 N	—	[22]
PVDF/NiO@SiO_2	Nanoparticles	Flat film	53 V @ 0.3 MPa	0.3 $\mu A{\cdot}cm^{-2}$ @ 0.3 MPa	685 $W{\cdot}m^{-3}$	[23]
PVDF	—	Electrospun membrane	48 V @ 8.3 kPa	6 μA @ 8.3 kPa	51 μW	[24]
PVDF/ZnO	Nanorods	Electrospun membrane	85 V	2.2 μA	—	[25]

Table 1.
Comparison of the PVDF-based nanogenerator performance. The experimental conditions such as applied force, operation mode, area of nanogenerator, and load resistance were different in the literature.

process [8–11]. The limitation of PVDF-based nanogenerators has been their low power generation capacity. Hence, many research groups have studied to enhance the performance of nanogenerators, by utilizing various fabrication methods, and structures, by incorporating fillers (**Table 1**).

In this chapter, we discuss different fabrication techniques and developments of PVDF-based nanogenerators in detail. This book chapter is organized as follows. In Section 2, we introduce PVDF and its copolymers with their properties. In Section 3, we focus on fabrication methods used to prepare PVDF-based nanogenerators. In Section 4, we briefly cover conventional PVDF film-based nanogenerators. In Section 5, we review composite-based nanogenerators and how certain factors affect their performance of the nanogenerators. In Section 6, we introduce the energy sources that can be harvested by the nanogenerators. In Section 7, we review the biocompatibility of PVDF and related works.

2. PVDF and its copolymers

Semicrystalline PVDF has at least four crystalline modifications: α, β, γ, and δ [26]. Generally, the α-phase is the most stable crystal phase of PVDF in ambient conditions. The conformation of α-PVDF, displayed in **Figure 1a**, is trans-gauche-trans-gauche (TGTG'). The α-phase is nonpolar because of its centrosymmetric symmetry and can be easily obtained from melt crystallization at atmospheric pressure. On the other hand, the β-phase is classified as a ferroelectric and exhibits the largest remnant polarization of ~ 13 μC/cm^2 among the phases. Ferroelectricity in the β-PVDF is directly correlated to its macroscopic dipole moment. In the β-phase,

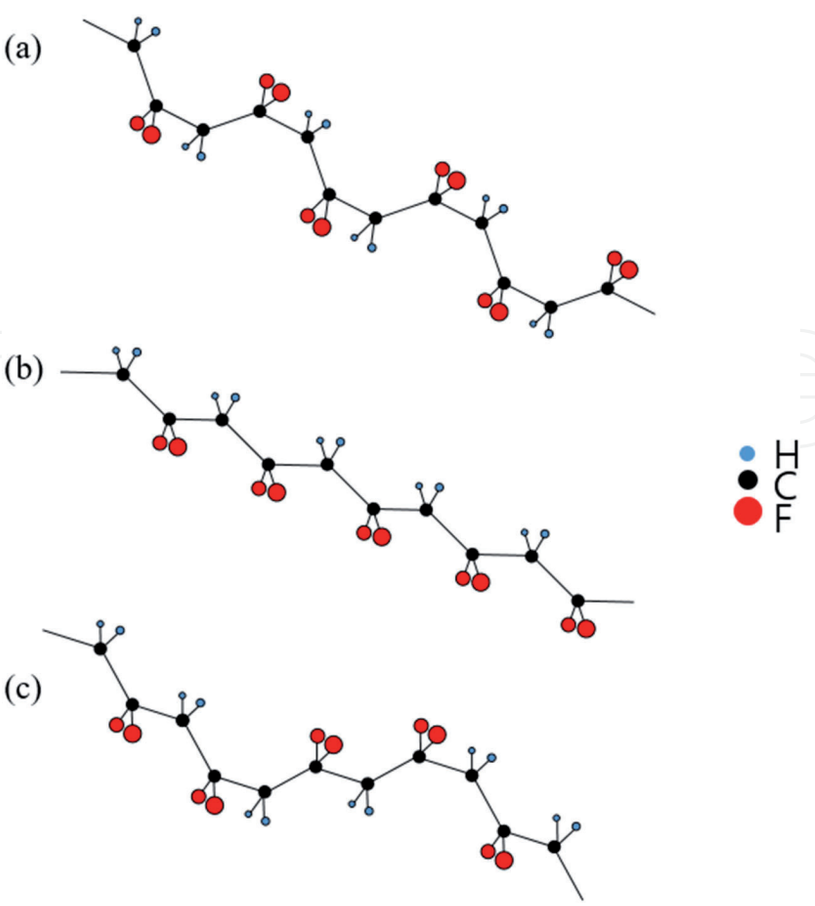

Figure 1.
Configuration in the unit cell of (a) the α-phase, (b) the β-phase, and (c) the γ-phase.

the conformation is all trans (TTTT) as shown in **Figure 1b**. The transition from the PVDF α-phase to the β-phase can be induced by stretching the polymer. The γ-phase is also polar and its conformation is trans-trans-trans-gauche-trans-trans-trans-gauche (T_3GT_3G) as shown in **Figure 1c**. The γ-phase is also ferroelectric. However, the γ-phase is less frequently observed because it requires extreme temperature control and high pressures to develop. The δ-phase has the same configuration as the α-phase. The difference is that the δ-phase is a ferroelectric. Crystallization of the δ-phase can be achieved by electroforming from the bulk α-PVDF in a high electric field of about 170 MV/m. Recently, M. Li *et al*. demonstrated that a δ-PVDF thin film can be made at elevated temperatures by applying a short pulse of about 250 MV/m [27]. They confirmed the existence of the δ-phase via combined GI-XRD and FTIR measurements on pristine and electroformed capacitors.

Due to its electroactive properties, high β-phase content is desirable for applications. This can be achieved physically or chemically. The most common chemical derivatives of PVDF available are polyvinylidene fluoride-trifluoroethylene (P(VDF-TrFE)) and polyvinylidene fluoride-hexafluoropropene (P(VDF-HFP)). Despite its high cost, P(VDF-TrFE) is often preferred over PVDF. The main advantage of P(VDF-TrFE) is that the β-phase can easily develop without mechanical stretching or incorporating fillers. The mechanism behind the development of the β-phase is based on the introduction of additional fluorine atoms within a certain amount, which allows steric hindrance to occur. P(VDF-HFP) has received a lot of attention because of its extremely high electrostrictive response [28]. As with PVDF, the β-phase in P(VDF-HFP) can be obtained by mechanical stretching [29]. Another way to develop the β-phase in P(VDF-HFP) is casting from solution in dimethylformamide (DMF) [30].

Since the discovery of piezoelectricity in PVDF [31], the mechanism behind the piezoelectric response has been a subject of debate. Recently, L. Katsouras *et al*. identified the piezoelectric effect in semicrystalline PVDF and its copolymers via *in-situ* dynamic X-ray diffraction, from measurements with P(VDF-TrFE) capacitors [32]. The piezoelectric effect is attributed to the change in lattice constant produced by the electromechanical coupling between the intermixed crystalline and amorphous regions as well as the electrostrictive response of the crystalline part. Both the electrostrictive Q_{33} and the additional, $d_{coupling}$, are negative; hence, the piezoelectric coefficient, d_{33}, of P(VDF-TrFE) is negative. Understanding the fundamental basis of piezoelectricity in ferroelectric polymers is essential to further technological innovations.

In order to identify the phases of PVDF, analysis techniques based on electromagnetic radiations such as X-ray and infrared have been widely used. The crystalline structure in PVDF and its copolymers can be confirmed via X-ray diffraction (XRD). In general, the nonpolar α-phase and the polar β- and γ-phases of PVDF appear in XRD patterns (**Figure 2a**) [33]. There are peaks at 18.4, 19.9, and 26.6° corresponding to (020), (110), and (021) reflections of the monoclinic α-phase, respectively. The peak at 20.6° is associated with the crystalline (200) and (110) of the orthorhombic β-phase. For the γ-phase, the dominant peaks appear at 18.5 and 20.2° corresponding to (020) and (110), respectively. In the case of P(VDF-TrFE), the peak corresponding to the (200) and (110) planes of the β-phase crystalline phase is represented at 19.7°. The position and width of peaks can change depending on experimental conditions and the ratio between VDF and TrFE. Therefore, the diffraction patterns can be differently observed in the literature.

The ferroelectric phase formation of PVDF and its copolymers have been also confirmed using Fourier transform infrared spectroscopy (FTIR). However, there exists a conflict on spectrum peaks corresponding the phases. Recently, X. Cai *et al*. documented reports on the vibrational bands of PVDF materials via FTIR to shed

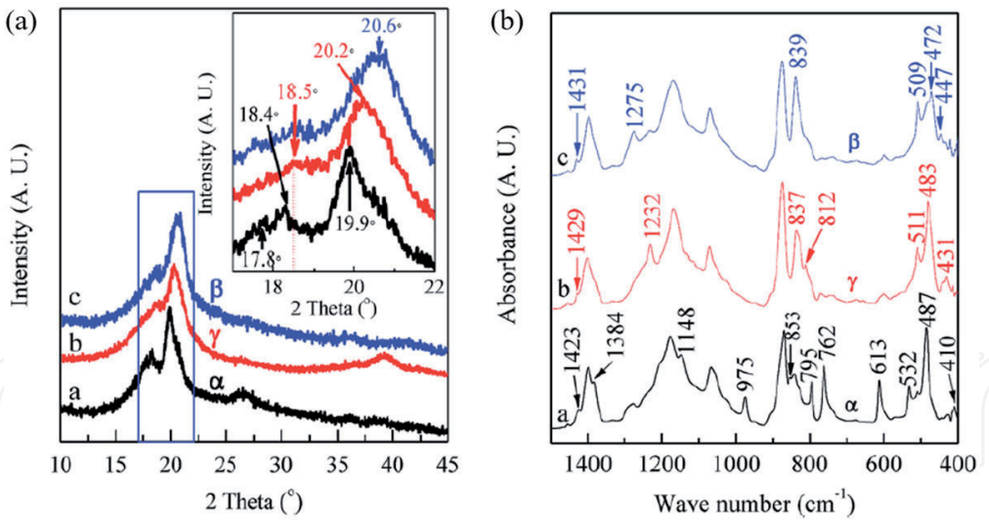

Figure 2.
XRD patterns (A) and FTIR spectra (B) of PVDF membranes [33].

light on this issue [33]. Furthermore, they analyzed the FTIR results and suggested the relative fraction of the β- and γ-phase calculations in terms of crystalline components as shown in **Figure 2b**. Since the absorption band at 840 cm^{-1} corresponds to the β, γ, or both phases, the fraction of the β- and γ-phases can be calculated as follows:

$$F_{EA} = \frac{I_{EA}}{\left(\frac{K_{840}}{K_{763}}\right) I_{763} + I_{EA}} \times 100\% \tag{1}$$

where I_{EA} and I_{763} are the absorbance at 840 and 763 cm^{-1}, respectively, and K_{840} and K_{763} are the absorption coefficients at the respective wave numbers, whose values are 7.7×10^4 and 6.1×10^4 cm^2 mol^{-1}, respectively. If PVDF materials contain both phases, another method is needed to quantify individual β- and γ-phases. The quantification of β- and γ-phases can be demonstrated as follows:

$$F(\beta) = F_{EA} \times \left(\frac{\Delta H_{\beta'}}{\Delta H_{\beta'} + \Delta H_{\gamma'}}\right) \times 100\% \tag{2}$$

$$F(\gamma) = F_{EA} \times \left(\frac{\Delta H_{\gamma'}}{\Delta H_{\beta'} + \Delta H_{\gamma'}}\right) \times 100\% \tag{3}$$

where $\Delta H_{\beta'}$ and $\Delta H_{\gamma'}$ are the height differences (absorbance differences) between the peak around at 1275 cm^{-1} and the nearest valley around at 1260 cm^{-1}, and the peak around 1234 cm^{-1} and the nearest around at 1225 cm^{-1}, respectively.

3. Fabrication techniques

PVDF and its copolymer-based nanogenerators consist of a layer of PVDF or its copolymers sandwiched between two electrodes, like a capacitor. As previously noted, PVDF and its copolymer-based nanogenerators have advantages over piezoelectric ceramics-based nanogenerators, because of their flexibility and high piezoelectric voltage coefficient (g_{33}). One important consideration is the choice of a suitable technique for the fabrication of ferroelectric polymer-based nanogenerators. A great variety of methods to make ferroelectric polymer-based nanogenerators has been developed for a few decades: solution casting, spin coating, template-assisted method, electrospinning, thermal drawing, and dip coating, as

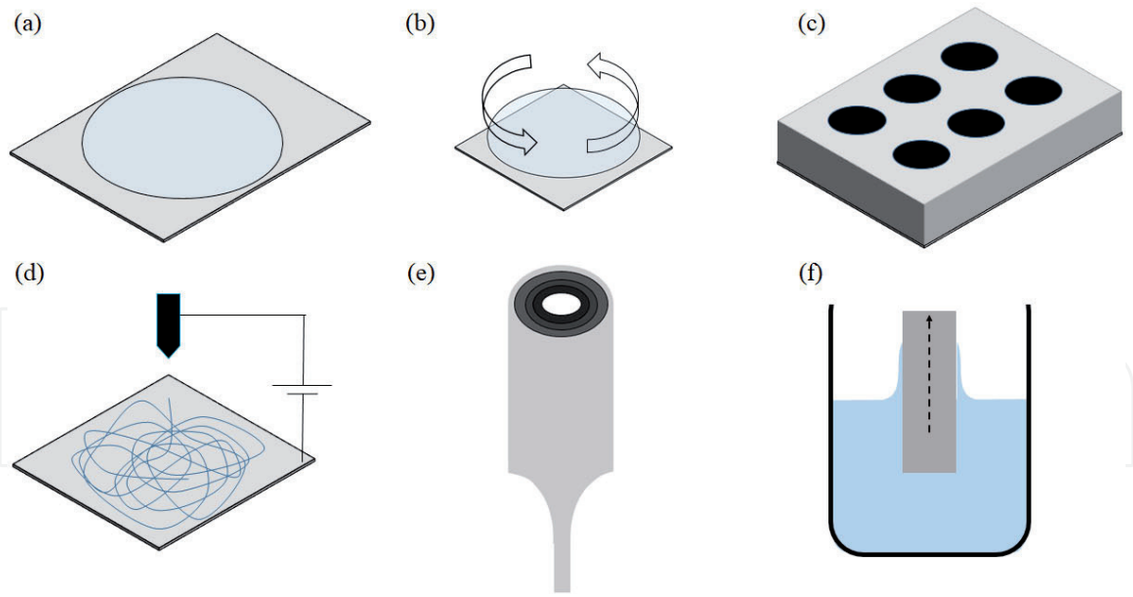

Figure 3.
Schematic drawing of fabrication methods of PVDF-based nanogenerator. (a) Solution casting, (b) spin coating, (c) template-assisted method, (d) electrospinning, (e) thermal drawing, (f) dip coating.

described in **Figure 3** [9, 12, 34–38]. The particular fabrication technique can affect the crystallinity and phase of ferroelectric polymers, influencing their electroactive and mechanical properties. This section covers conventional and recently developed fabrication techniques involving ferroelectric polymers in greater detail.

3.1 Solution casting

Usually, PVDF and its copolymer-based nanogenerators are prepared by solution casting because it is a simple and low-cost process and allows large-scale production. The casting method is also suitable for preparing composites of fillers and a polymer matrix because it is relatively insensitive to the viscosity and density of solution. As a result, solution casting has been used in most research on composite-based nanogenerators [16, 18, 22, 23, 39]. The thickness of the film can be controlled by the type of organic solvents employed and the concentration and amount of the ferroelectric polymer solution. Since evaporation speed can differ depending on the organic solvents used, the morphology of the ferroelectric polymer films can also be affected [40].

3.2 Spin coating

Spin coating is a universally used technique to fabricate uniform thin polymer films using the centrifugal forces induced by a spinning substrate. The thickness of the films can be controlled by a few parameters, such as solution concentration, viscosity, spin speed, and spin time. Generally, a low concentration polymer solution (<10%) is used for uniformity. In addition, the thickness of spin-coated ferroelectric polymer films can be controlled by the number of successive spin coatings.

Spin coating has been successfully used to prepare nanogenerators based on thin P(VDF-TrFE) films. For example, Z. Pi *et al*. reported a flexible nanogenerator based on P(VDF-TrFE) thin film produced by spin coating. A 2% concentration of P(VDF-TrFE) copolymer solution was repeatedly spin coated on the substrate to reach the required thickness [12]. In another study, Lee *et al*. successfully developed a nanogenerator based on micropatterned P(VDF-TrFE) polymer (thickness ≈7 μm) [41].

They evaluated the improved stretchability, mechanical durability, and robustness of the line-based micropatterned nanogenerator, compared to a flat (nonpatterned) nanogenerator.

3.3 Template-assisted method

Nanoconfinement involves confining dimensional geometries in a nanosized region. Typically, the template-assisted method from a melt or solution has been employed to fabricate one-dimensional nanostructures [8, 9]. In the template-assisted method, a polymer melt or solution is used to wet the surface of a porous template. It permeates into the pore of the template due to the high surface energy of the template walls. Finally, polymer nanotubes or nanowires form with a uniform size distribution. This technique has been reported to improve the performance of polymer-based nanogenerators. For example, V. Bhavanasi *et al*. prepared P(VDF-TrFE) nanotubes using a template-assisted method, with a P(VDF-TrFE) melt and anodic aluminum oxide (AAO) templates with a pore diameter of 200 nm [42]. The resulting P(VDF-TrFE) nanotubes demonstrated high power generation under dynamic compression pressure compared to that of P(VDF-TrFE) films. This improved performance was attributed to the enhanced piezoelectric coefficients, strain confinement in the 1D geometry, and improved surface area.

The nanoconfinement via templates induces ferroelectric polymer nanowires to retain preferential orientation with the b-axis parallel to the long axis of the template. This orientation leads to a vertical direction of the polarization parallel to the channel axis. Y. Calahorra *et al*. investigated the electromechanical interactions in individual P(VDF-TrFE) nanowires via piezoresponse force microscopy (PFM) [43]. Their results indicate that P(VDF-TrFE) nanowires grown via template-assisted methods possess piezoelectric properties without electrical poling process, which is called as "self-poled." However, the d_{33} coefficient of nanowires without poling was lower than that of nanowires with poling. After tip-induced electrical poling, the d_{33} of the nanowires increased from 7.7 pm/V to 21.6 pm/V. This phenomenon can be attributed to the direction of polarization parallel to the substrate before electrical poling.

When a template-assisted method is used, in-situ poling can be applied at the same time. This is known as the template-assisted electricity-grown method. X. Chen *et al*. fabricated vertically well-aligned P(VDF-TrFE) nanowire arrays with a preferential polarization orientation [44]. The contents of the β-phase in P(VDF-TrFE) nanowires and bulk films were analyzed via Fourier transform infrared (FTIR) measurement. The percent content of β-phase in the P(VDF-TrFE) nanowires increased to 83.5%. This value was higher than the bulk films (75.2%). Without further poling, the P(VDF-TrFE) nanowire array delivered an output voltage about 9 times higher than conventional spin-coated bulk films.

3.4 Electrospinning

Electrospinning is another common method used to fabricate β-phase ferroelectric fibers without further mechanical stretching or electrical poling processes [45]. The electrospinning technique utilizes an electrical force to obtain fibers. The basic principle of conventional electrospinning is as follows: When a DC electric field is applied between the spinneret (metallic needle) and the collector (grounded conductor), a conical object called a Taylor cone forms at the tip of the needle. When the electric field rises above a threshold value, the resulting electrostatic force can overcome the surface tension and viscous force of the polymer solution. An electrified liquid jet ejected from the nozzle undergoes a stretching and whipping process

and then splits into threads with diameters ranging from hundreds of micrometers to tens of nanometers.

In 2011, D. Mandal *et al*. prepared P(VDF-TrFE) nanofiber webs via electrospinning [37]. They found evidence of the preferential orientation of CF_2 dipoles in the P(VDF-TrFE) nanofiber web via analyses using polarized FTIR and piezoelectric signal. They also demonstrated that output current signal could be enhanced by stacking several tens of layers of the electrospun web with the same polarization.

Unlike conventional electrospinning, near-field electrospinning using a short needle-to-collector distance enables superior location control, to produce orderly nanofiber patterns over large areas [46]. Notably, C. Chang *et al*. utilized a direct-write technique by means of near-field electrospinning (NFES) to produce and place piezoelectric PVDF nanofibers on working substrates [47]. They measured the piezoelectric response of single PVDF nanofibers to calculate their energy conversion efficiency (ECE). The ECE was defined as

$$ECE = \frac{Electric\ energy\ generated}{Mechancial\ energy\ applied} = \kappa^2 \tag{4}$$

where κ is the electromechanical coupling coefficient of the piezoelectric material. The electric energy W_e was estimated by integrating the product of the output voltage and current of the PVDF nanogenerator when stretched. The elastic strain energy was estimated using

$$W_s = \frac{1}{2} EA\,\varepsilon^2 L_0 \tag{5}$$

where E is the Young's modulus of the material, A is the cross-sectional area, ε is the strain applied to the material, and L_0 is the length of the material. It was found that the energy conversion of the nanofiber-based nanogenerator (average 12.5%) was higher than experimental PVDF films (0.5–4%) and conventional PVDF thin films (0.5–2.6%).

3.5 Thermal drawing

Another interesting method to make ferroelectric polymer fibers is thermal drawing, as reported by S. Egusa *et al* [38]. The advantage of thermal drawing is that all components (piezoelectric layer, electrode layers, and wrapping layer) are extracted a preform made of poly(vinylidene fluoride) with metal electrodes and an insulating polymer, making the process simpler compared to other methods. However, they encountered some challenges. During thermal drawing, there is a susceptibility to break up and mixing due to flow instabilities and variation in layer thickness. To address such challenges, they used carbon-loaded poly(carbonate) (CPC) and P(VDF-TrFE). CPC has high viscosity (10^5–10^6 Pa s) at the draw temperature and thus can be used to confine the low-viscosity crystalline piezoelectric layer and ensure adequate conductivity (1–10^4 Ω m). In the case of P(VDF-TrFE), the β-phase can form without any mechanical stress compared to PVDF. Therefore, they were able to make multimaterial piezoelectric fibers with a uniform diameter using these two materials. They also demonstrated the benefits of drawing ferroelectric polymer fibers for application in acoustic transducers and capacitors [38, 48]. However, they did not mention the scavenging ability of P(VDF-TrFE) fiber prepared by thermal drawing.

Due to flexibility of the thermal drawing, it has been successfully demonstrated for fabricating composite fibers such as $BaTiO_3$-PVDF, $Pb(Zr,Ti)O_3$ (PZT)-PVDF, and carbon nanotube (CNT)-PVDF [49]. In that study, the piezoelectric performance of the fabricated fibers was systematically compared while bending and

releasing. For a $BaTiO_3$-PVDF fiber, the generated open-circuit voltage and short-circuit current were 1.4 V and 0.8 nA, respectively. For a PZT-PVDF fiber, the corresponding values were 6 V and 4 nA. A CNT-PVDF fiber generated 3 V and 1.2 nA. These results were attributed to the high piezoelectric coefficient ($BaTiO_3$ and PZT) or the induced β-crystallization (CNT).

3.6 Dip coating

Dip coating is one of the most effective methods of depositing ferroelectric polymers on a 3D substrate. For example, D. Kim *et al*. developed a three-dimensional spring-type nanogenerator using a dip-coating and multidirectional electrode deposition [35]. The nanogenerator had a bi-layered structure with a top electrode and a P(VDF-TrFE) layer on a conventional spring that had two roles. It served as both the core electrode and the mechanical substrate for the ferroelectric polymer. In another study, J. Ryu *et al*. fabricated a P(VDF-TrFE)/polydimethylsiloxane (PDMS) stretchable hollow fiber using dip coating [36]. To fabricate the fiber, a cylindrical carbon rod was used as a template, onto which each of the layers was sequentially coated. The diameters of the P(VDF-TrFE)/PDMS layer and PDMS layer were controlled by varying the withdrawal speed during dip coating.

4. Nanogenerators based on pure PVDF films

The typical type of nanogenerator is based on ferroelectric polymer films without any further processing or incorporation of fillers. Conventional PVDF film-based nanogenerators can be simply fabricated and easily stacked to improve performance. In addition, the flexible nanogenerators can be designed using various structures. For example, J. Zhao and Z. You fabricated a nanogenerator based on specially designed sandwich structure that was compatible with a shoe [50]. The structure was composed of multilayered PVDF films and two wavy surfaces of a movable upper plate and a lower plate. The PVDF film layers were connected in parallel for high output current. Due to the structural design and stacked PVDF films, the nanogenerator provided an average output power of 1 mW while walking at a frequency of ~1 Hz. In another study, W.-S. Jung *et al*. prepared a curved piezoelectric nanogenerator consisting of multilayered PVDF films and a polyimide substrate [13]. They also connected all PVDF films in parallel to increase the output current. The curved structure enhanced the output power by distributing effectively applied stress. The authors integrated the nanogenerator into a shoe-insole and to a watch strap and attached them to long-sleeved shirts, and then evaluated the PVDF-based nanogenerators as a power source for wearable sensors and biomedical devices.

5. Nanogenerators based on composites

In order to enhance the electrical and mechanical properties of ferroelectric materials, many research groups have employed the concept of composites, typically made of a polymer and a ceramic. Composite is a common approach in piezoelectric-based applications. Ultrasonic transducer is a typical example. The composites are used for impedance matching. Since piezoelectric ceramics like PZT, $BaTiO_3$, and $Pb(Mg_{1/3}Nb_{2/3})O_3$-$PbTiO_3$ (PMN-PT) have a relatively high acoustic impedance compared to water or human tissue, impedance matching is required. Such matching results in broad bandwidth and increased sensitivity.

Composites can also be utilized for nanogenerators based on PVDF and its copolymers to boost their performance. The outputs of nanogenerators depend on a variety of factors, which include the piezoelectric coefficient, elastic modulus, and dielectric constant. The output voltage generated by nanogenerators can be expressed as

$$V_{out} = \int g_{33}\varepsilon(l)Edl \tag{6}$$

where $\varepsilon(l)$ is the strain, E is the elasticity modulus, and g_{33} is the piezoelectric voltage constant, given by $g_{33} = \frac{d_{33}}{\varepsilon_0 \varepsilon_r}$ with d_{33} being the piezoelectric coefficient, ε_r being the dielectric constant, and ε_0 being the permittivity of free space [15]. Hence, a higher piezoelectric coefficient and elastic modulus, and a lower dielectric constant result in higher nanogenerator performance. In this section, we will discuss the effect of fillers on composite-based nanogenerators. By varying the concentration, size, and morphology of fillers, the factors of composites can be controlled.

5.1 Piezoelectric coefficient

A piezoelectric coefficient is the most critical factor affecting the performance of nanogenerators. The piezoelectric coefficient (d_{33}) of bulk PVDF and its copolymers is remarkably low compared to that of bulk ceramics such as PZT (700 pC/N) [51], $BaTiO_3$ (350 pC/N) [52], and $Pb(Zn_{1/3}Nb_{2/3})O_3$-$PbTiO_3$ (PZN-PT) (2500 pC/N) [53]. As already mentioned in Section 2, the piezoelectric coefficient of PVDF and its copolymers is related to their crystallinity. In other words, the performance of nanogenerators can be improved by increasing the crystallinity of the ferroelectrics.

Recent studies have revealed that the crystallinity of ferroelectric polymers can change with fillers including organics, inorganics, and metals [16, 23, 39, 54]. The amount of β-phase in ferroelectric polymers can be enhanced by imbedding fillers into the ferroelectric polymer. For example, B. Dutta *et al*. reported a piezoelectric nanogenerator based on a $NiO@SiO_2$/PVDF nanocomposite [23]. To prevent agglomeration, they coated nonconductive SiO_2 on the NiO nanoparticles, which resulted in the homogeneous dispersion of the nanofillers in the polymer matrix. FTIR results indicated that the β-phase in the PVDF increased with the increasing loading fraction of $NiO@SiO_2$ as shown in **Figure 4a**. This phenomenon occurred due to the electrostatic interaction between the negatively charged surface of the $NiO@SiO_2$ nanoparticles and the positive $–CH_2$ groups of PVDF.

In addition to considering the content of fillers, the geometric structures of fillers should be also considered for their effect on the extent of β-phase crystallization and their influence on piezoelectric performance in the composites. A recent example was demonstrated in Ag/PVDF composites, where the effect of mixing silver fillers with different morphologies into P(VDF-TrFE) was investigated [54]. When Ag nanoparticles were added to P(VDF-TrFE), the crystalline transformation of P(VDF-TrFE) was not observed (**Figure 4b**). Similarly, work conducted by H. Paik *et al*. also found that the effect of adding Ag nanoparticles has an insignificant effect on the internal structures of the film [55]. On the other hand, when Ag nanowires with a diameter of 120 nm were mixed with P(VDF-TrFE), some α-phase transformed into β-phase, which indicates that the piezoelectric response can be enhanced as shown in **Figure 4c**. This was attributed to the fact that the molecular structure of P(VDF-TrFE) can be easily packed in a form that favors the formation of β-phase due to the planar surface of the Ag nanowires.

Interestingly, many research groups have used ferroelectric materials as fillers to enhance the performance of their nanogenerators. Even though ferroelectric fillers

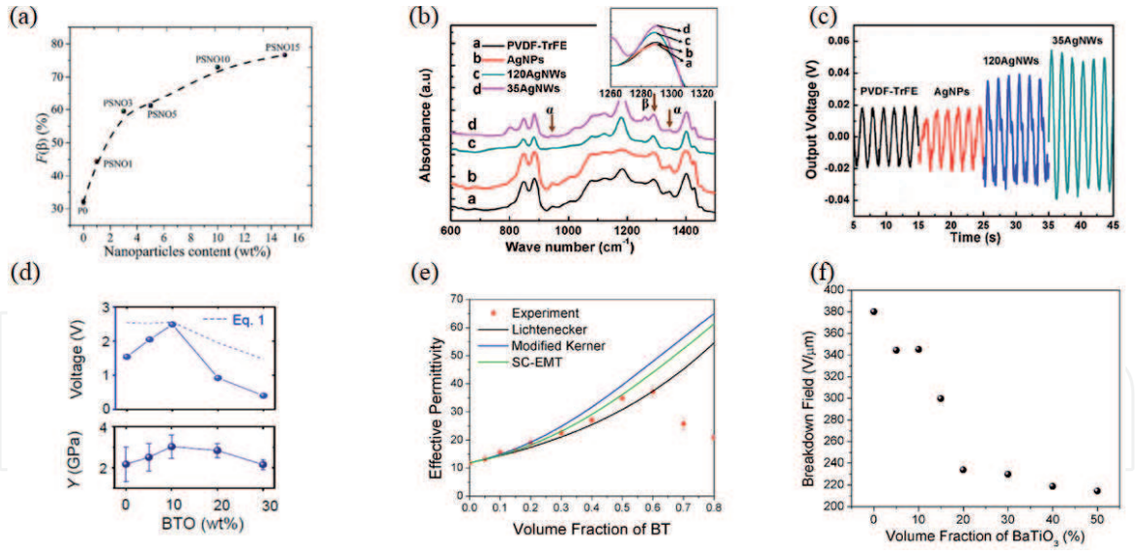

Figure 4.
(a) Variation of β-phase fraction (F(β)) with NiO@SiO_2 nanoparticles loading in PVDF matrix. Reproduced with permission [23]. Copyright 2018, American Chemical Society, (b) FTIR spectra of P(VDF-TrFE) film blended with different Ag nanocomposites. (the small picture was zoom-in view of peak intensity at 1290 cm^{-1}). (c) the piezoelectric response of P(VDF-TrFE) with different Ag nanofillers. Reproduced with permission [54]. Copyright 2016, Elsevier. (d) Comparison of the piezoelectric outputs with measured Young's modulus. Reproduced with permission [58]. Copyright 2018, MDPI. (e) Comparison of measured effective relative permittivity (at 1 kHz) of nanocomposites as a function of PFBPABT nanoparticle volume fraction with predicted values from different theoretical models. (f) the breakdown strengths (failure probabilities: 63.2%) at each volume fraction as determined from the Weibull analysis. Reproduced with permission [60]. Copyright 2018, American Chemical Society.

such as particles, nanowires, and nanorods have a poor piezoelectric coefficients, compared to that of bulk ceramics, they are still good candidates for piezoelectric nanogenerators. For example, PMN-PT nanofiber has a piezoelectric coefficient (d_{33}) of 50 pC/N [56].

However, PVDF and its copolymers have a negative piezoelectric coefficient, as previously mentioned. If PVDF and its copolymers are used as matrices, the conflict of piezoelectric constants can limit its advantages and result in lower output. Previous reports indicated that PZT/P(VDF-TrFE) 0–3 composites with 50 volume percent ceramic did not exhibit a piezoelectric response because they had the opposite sign piezoelectric coefficient, thus canceled out [57]. To circumvent this effect, different poling process can be adapted. For example, C. K. Jeong *et al*. demonstrated an enhanced nanogenerator based on $BaTiO_3$ nanowires and P(VDF-TrFE), which was poled using double-side poling process to remove the piezoelectric discrepancy between $BaTiO_3$ and P(VDF-TrFE) [21]. These examples further highlight why the mechanism behind the combination of piezoelectric nanofillers and piezoelectric polymers should be comprehensively explored.

5.2 Elastic modulus

It is also important to consider elastic modulus, the resistance to elastic deformation under load, according to the equation (Eq. (6)). A recent publication showed that Young's modulus plays an important role in a piezoelectric nanogenerator [58]. In that work, H. S. Kim *et al*. used paraelectric $BaTiO_3$ nanoparticles as fillers to exclude the effect from the piezoelectricity of the fillers. The Young's modulus increased from 2.17 to 3.03 GPa when the BTO content increased from 0 to 10 wt% and then decreased to 2.15 GPa as the content further increased to 30 wt% (**Figure 4d**). They found that the BTO content-output relationship was directly related to Young's modulus. Clearly, the optimal content for achieving the

maximum Young's modulus, which corresponds to the highest piezoelectric output, should be identified.

5.3 Dielectric constant

Dielectric constants are an important parameter that also can affect the performance of nanogenerators. In composites, the dielectric constant can change with the volume of fillers. In a $BaTiO_3$-PVDF composite film, the dielectric constant increased from 8 to 31.8 at a frequency of 10^4 kHz when the volume fraction of fillers was increased from 0–30% [59]. Furthermore, the size of the nanoparticles can modify the dielectric properties. When the BaTiO3 filler size was increased from 10.5 to 34.6 nm, the dielectric constant at a frequency of 10^4 kHz increased from 20.1 to 31. In another study, P. Kim *et al*. systematically studied the dielectric constant and dielectric breakdown strength of a composite comprising P(VDF-HFP) and phosphoric acid surface-modified $BaTiO_3$ nanoparticles [60]. The dielectric constant increased as the nanoparticle volume fraction was increased from 0–60% and then decreased as the nanoparticles volume fraction increased above 60% (**Figure 4e**). The drop in dielectric constant at high volume fractions was attributed to the effect of the porosity of the composites. The dielectric breakdown strength decreased when the nanoparticle volume fraction increased, due to percolation of the $BaTiO_3$ nanoparticles and air voids (**Figure 4f**).

6. Energy sources

In addition to mechanical deformation, such as uniaxial compression and bending, energy sources such as air flow, sound, and thermal fluctuation are also available. A typical example of ambient natural sources is wind. Ferroelectric polymer-based nanogenerators can easily yield electricity from wind energy because of their considerable flexibility. For example, Li *et al*. fabricated nanogenerators based on P(VDF-TrFE) films to harvest mechanical energy from low speed wind, which is very close to winds commonly observed in the natural environment [34]. The experimental setups are illustrated in **Figure 5a**. They evaluated the wind energy extraction capability by comparing three instinct operating modes. Each operating modes exhibited different piezoelectric energy harvesting behaviors, including mode frequency, output voltage, and power. The authors concluded that a nanogenerator operating where the wind is incident to the side of the film delivered high output power compared to other modes within the wind speed range of 1.7 and 4.7 m/s (**Figure 5b**). These results may be attributed to the huge deflection that occurred over the entire area of the nanogenerator.

Besides wind, sound is also an abundant energy source that can be found in the environment. PVDF films can be used as an active layer for harvesting sound waves. A variety of polymer-based nanogenerators have been developed to scavenge energy from sonic inputs. For example, S. Cha *et al*. presented nanoporous arrays of PVDF fabricated by a lithography-free, template-assisted preparation method (**Figure 5c**) [61]. They demonstrated that the porous PVDF nanogenerators generated an output voltage and current of 2.6 V and 0.6 μA, respectively. These output values were 5.2 times and 6 times higher than bulk PVDF film nanogenerators, respectively (**Figure 5d**). The piezoelectric potential was enhanced in the nanoporous structure as a result of the geometrical strain confinement effect.

More recently, nanoweb-type nanogenerators were developed to convert sound wave into electrical energy [62, 63]. The benefit of using nanowebs in nanogenerators compared to films is their high power generation because they are more flexible and easier to vibrate under the same acoustic waves.

Pyroelectricity is a property of certain materials, which develop an electric field across the polar axis when there is a temperature change. According to the pyroelectric theory [64], the pyroelectric current I is expressed as

$$I = \frac{dQ}{dt} = S\lambda\frac{dT}{dt} \tag{7}$$

where Q, S, λ, and$T$ are the induced charge, the electrode surface of the material sample, the pyroelectric coefficient, and the temperature, respectively. Ferroelectric ceramics like PMN-PT and PZT have high pyroelectric coefficients above 550 $\mu Cm^{-2} K^{-1}$ compared to those of ferroelectric polymers ($33\mu Cm^{-2} K^{-1}$). As a result, a PZT-based nanogenerator delivered more current density than that of ferroelectric polymers. However, PVDF and its copolymers have also been employed to harvest thermal energy from temperature fluctuations, where they provide the benefits of light weight, low-cost, lead-free, flexible, and transparent

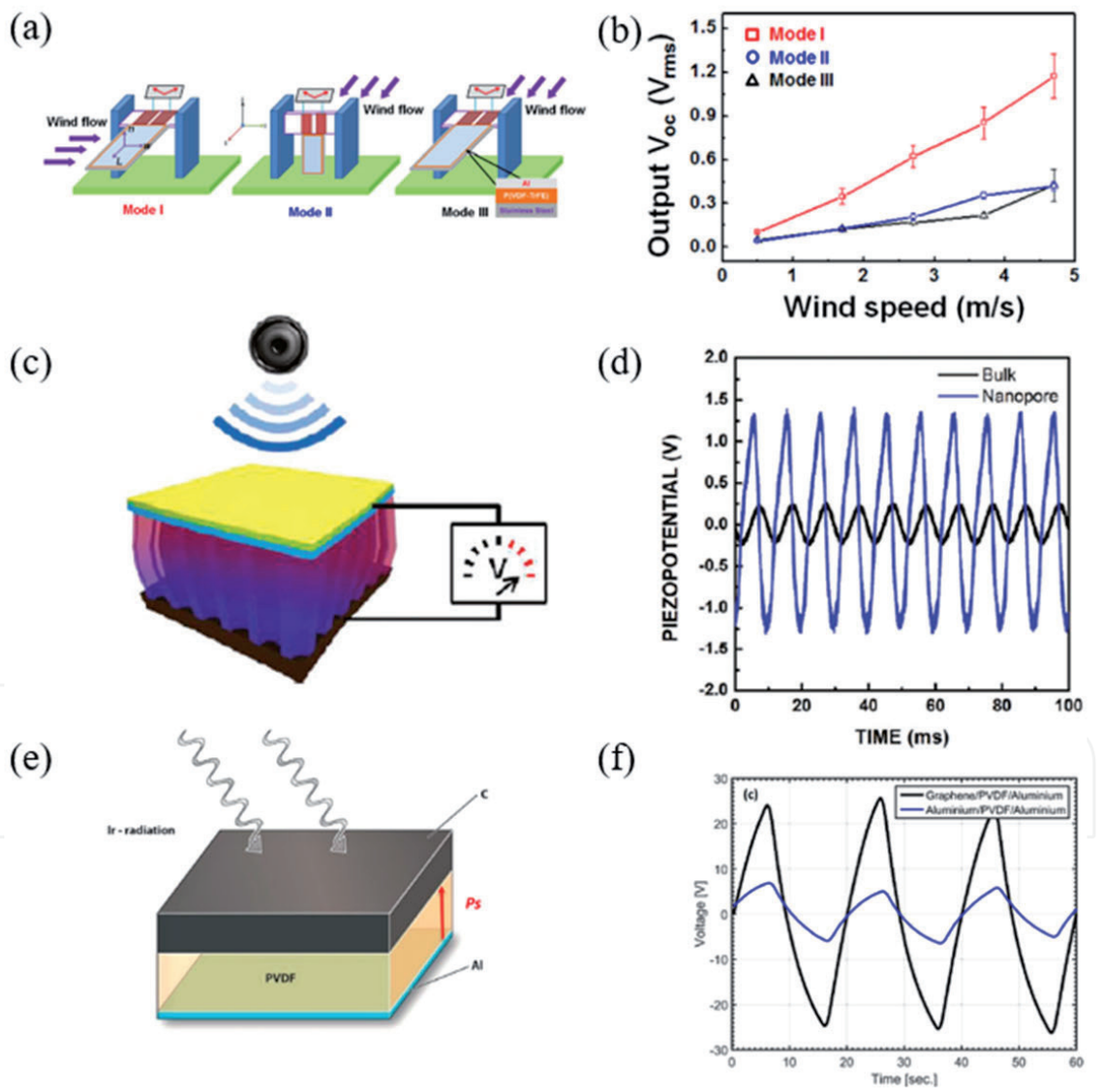

Figure 5.
(a) Schematic illustration of three different operation modes: Mode I, mode II, and mode III. (b) Output voltage (Vout) as a function of incident wind speed within the range of 0.5–4.7 m/s for modes I, II, and III. Reproduced with permission [34]. Copyright 2014, AIP publishing. (c) Schematic depiction of the potential of porous nanogenerators generated by the sonic wave. (d) Piezoelectric potential from the porous PVDF and bulk structure under the same force. Reproduced with permission [61]. Copyright 2011, American Chemical Society. (e) Schematic illustration of a PVDF/graphene ink pyroelectric device. (f) Open-circuit voltage for aluminum electrode and PVDF/graphene ink pyroelectric energy harvesting device. Reproduced with permission [68]. Copyright 2017, American Chemical Society.

properties [41, 65, 66]. A number of research groups have focused on improving the performance of such nanogenerators by changing their designed conditions. For example, D. Zabek *et al*. reported a simple modification of the electrode design in a PVDF-based nanogenerator [67]. The partially covered electrode was developed by photo-lithography and a wet etching process. The modification of the electrode design enabled a significant increase in pyroelectric voltage (380%), current (480%), and pyroelectric energy harvesting transformation (1080%).Their findings showed that the electrode area coverage could be optimized by balancing the ratio of the area of aluminum electrode required to get the free charge to the area of exposed PVDF to improve heat transfer. In another study, they also demonstrated that interconnected graphene nanoplates (GNPs) can be used as an electrode for high thermal radiation absorbance and high electrical conductivity as shown in **Figure 5e** [68]. The GNPs were easily deposited by a screen print technique. The graphene ink/PVDF/Al system showed better performance than a system with conventional aluminum electrodes (**Figure 5f**).

7. Biocompatibility

Lead (Pb) is considered one of the core materials in modern society because it is inexpensive and has high density and resistance to corrosion. However, it is also toxic and can harm multiple human body systems. Legislation has been adopted in many countries to prevent and reduce the use of Pb in many communities [69]. Currently, many of the materials with high piezoelectric performance are lead-based materials, that is, $PbTiO_3$, $Pb(Zr,Ti)O_3$, PMN-PT, $Pb(Mg_{1/3}Nb_{2/3})O3$-$Pb(Zr,Ti)O_3$ (PMN-PZT), and PIN-PMN-PT [70–72]. They are used in a wide variety of applications including sensors, actuators, and ultrasonic transducers. The EU's Restriction of Hazardous Substances (RoHS) Directive of 2002 and its revision (RoHS 2) in 2011 designated certain piezoelectric devices as exemptions since lead-free piezoelectrics cannot completely replace all lead-based piezoelectrics at this time [69]. Nevertheless, it is urgent to develop lead-free piezoelectrics that can perform as well as or better than PZT.

From the biocompatibility point of view, one of the most promising alternatives is a ferroelectric polymer. The unique advantage of PVDF and its copolymers lies in their good stability, similar to PTFE. They are chemically inert and resistant to sunlight [65, 73, 74]. There have been reports on the biocompatibility of PVDF-based nanogenerators. For example, Y. Yu *et al*. demonstrated biomechanical energy harvesting in a living organism using PVDF-based nanogenerator, where a

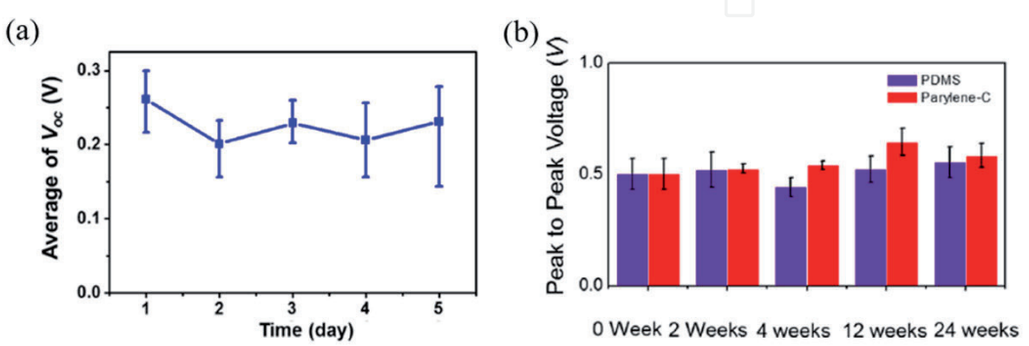

Figure 6.
(a) The variation of voltage output as a function of the testing period. Reproduced with permission [75]. Copyright 2016, Elsevier. (b) Stability of voltage outputs as a function of time for implantable NGs with different packaging strategies. The purple and red bars represent implantable NGs with PDMS and PDMS/Parylene-C package, respectively. Reproduced with permission [76]. Copyright 2018, Elsevier.

mesoporous PVDF film was encapsulated by polydimethylsiloxane (PDMS) [75]. They inserted the nanogenerator under the skin of a mice's leg and observed that there were no signs of incompatibility induced by the NG. In addition, an output voltage of 200 mV was stably generated from the gentle motions of the rat's leg for 5 days as shown in **Figure 6a**. In another work, J. Li *et al*. studied PDMS and PDMS/Parylene-C packaged PVDF nanogenerators implanted inside a female ICR mouse for up to 6 months [76]. They observed no signs of toxicity or incompatibility via pathological analyses and blood and serum test. In addition, there was no issue with reduction in electrical outputs over the entire implantation period (**Figure 6b**). Therefore, it is conceivable that PVDF-based nanogenerators can be used in a biological environment.

8. Conclusions

In this chapter, we summarized recent studies of ferroelectric polymer PVDF-based nanogenerators. PVDF and its copolymers are attractive materials for nanogenerator applications. The materials are flexible, transparent, chemically stable, easy to process, and biocompatible. Because of these advantages, PVDF-based nanogenerators can be placed anywhere, including bones, human skins, and wearable devices that usually have curved surfaces. In addition, they can harvest electricity from a variety of energy sources.

Considerable effort has been expended by numerous research groups to enhance the performance of PVDF-based nanogenerators using various fabrication methods, designing device structures, and incorporating fillers. However, studies on PVDF-based nanogenerators are fairly limited. The mechanisms leading to the enhanced performance after the incorporation of fillers should be comprehensively surveyed. Especially, in the case of ferroelectric fillers, a careful approach to the enhancement should be taken, since a piezoelectric effect also occurs with fillers. To optimize nanogenerator performance, circuits for nanogenerators should be developed. Their performance depends on the circuits and components, including load resistors, capacitors, and wiring. In order to realize the commercialization of PVDF-based nanogenerators, packaging of the devices is critical to prevent mechanical fatigue. The selection of substrates and electrode materials can also improve the mechanical properties of these devices. Therefore, the relationship between a ferroelectric polymer layer and other layers should be considered.

We hope that this chapter will help readers to better understand principles of PVDF-based nanogenerators. Furthermore, several new approaches that have been in this chapter can be adopted for other applications, such as sensors, actuators, and field-effect transistors.

Acknowledgements

This chapter is based on a research that has been conducted as part of the KAIST funded Global Singularity Research Program for 2019. Dr. Panpan Li was also supported by the Korea Research Fellowship Program funded by the National Research Foundation of Korea (no. 2017H1D3A1A01054478).

Author details

Jeongjae Ryu[1], Seongmun Eom[1], Panpan Li[1], Chi Hao Liow[1] and Seungbum Hong[1,2*]

1 Department of Materials Science and Engineering, Korea Advanced Institute of Science and Technology (KAIST), Daejeon, Republic of Korea

2 KAIST Institute of the NanoCentury, Korea Advanced Institute of Science and Technology, Daejeon, Republic of Korea

*Address all correspondence to: seungbum@kaist.ac.kr

References

[1] Ang L-M, Seng KP. Big sensor data applications in urban environments. Big Data Research. 2016;**4**:1-12. DOI: 10.1016/j.bdr.2015.12.003

[2] Palanisamy V, Thirunavukarasu R. Implications of big data analytics in developing healthcare frameworks—A review. Journal of King Saud University - Computer and Information Sciences. 2017;**31**(4):415-425. DOI: 10.1016/j.jksuci.2017.12.007

[3] Risteska Stojkoska BL, Trivodaliev KV. A review of internet of things for smart home: Challenges and solutions. Journal of Cleaner Production. 2017;**140**:1454-1464. DOI: 10.1016/j.jclepro.2016.10.006

[4] Attal F, Mohammed S, Dedabrishvili M, Chamroukhi F, Oukhellou L, Amirat Y. Physical human activity recognition using wearable sensors. Sensors (Basel). 2015;**15**:31314-31338. DOI: 10.3390/s151229858

[5] Hao Y, Foster R. Wireless body sensor networks for health-monitoring applications. Physiological Measurement. 2008;**29**:R27-R56. DOI: 10.1088/0967-3334/29/11/R01

[6] Lee Y-D, Chung W-Y. Wireless sensor network based wearable smart shirt for ubiquitous health and activity monitoring. Sensors and Actuators B: Chemical. 2009;**140**:390-395. DOI: 10.1016/j.snb.2009.04.040

[7] Yamada T, Hayamizu Y, Yamamoto Y, Yomogida Y, Izadi-Najafabadi A, Futaba DN, et al. Stretchable nanotube strain sensor for human-motion detection. Nature Nanotechnology. 2011;**6**:296-301. DOI: 10.1038/nnano.2011.36

[8] Kim D, Hong S, Hong J, Choi Y-Y, Kim J, Park M, et al. Fabrication of vertically aligned ferroelectric Polyvinylidene fluoride Mesoscale rod arrays. Journal of Applied Polymer Science. 2013;**130**:3842-3848. DOI: 10.1002/app.39415

[9] Oh S, Kim Y, Choi YY, Kim D, Choi H. No K, Fabrication of vertically well-aligned P(VDF-TrFE) nanorod arrays. Advanced Materials. 2012;**24**:5708-5712. DOI: 10.1002/adma.201201940

[10] Bune AV, Fridkin VM, Ducharme S, Blinov LM, Palto SP, Sorokin AV, et al. Two-dimensional ferroelectric films. Nature. 1998;**391**:874-877. DOI: 10.1038/36069

[11] Hu Z, Tian M, Nysten B, Jonas AM. Regular arrays of highly ordered ferroelectric polymer nanostructures for non-volatile low-voltage memories. Nature Materials. 2009;**8**:62-67. DOI: 10.1038/nmat2339

[12] Pi Z, Zhang J, Wen C, Zhang Z-B, Wu D. Flexible piezoelectric nanogenerator made of poly(vinylidenefluoride-co-trifluoroethylene) (PVDF-TrFE) thin film. Nano Energy. 2014;**7**:33-41. DOI: 10.1016/j.nanoen.2014.04.016

[13] Jung W-S, Lee M-J, Kang M-G, Moon HG, Yoon S-J, Baek S-H, et al. Powerful curved piezoelectric generator for wearable applications. Nano Energy. 2015;**13**:174-181. DOI: 10.1016/j.nanoen.2015.01.051

[14] Soin N, Shah TH, Anand SC, Geng J, Pornwannachai W, Mandal P, et al. Novel "3-D spacer" all fibre piezoelectric textiles for energy harvesting applications. Energy & Environmental Science. 2014;**7**:1670-1679. DOI: 10.1039/c3ee43987a

[15] Alluri NR, Saravanakumar B, Kim SJ. Flexible, hybrid piezoelectric film ($BaTi_{(1-x)}Zr_{(x)}O_3$)/PVDF

nanogenerator as a self-powered fluid velocity sensor. ACS Applied Materials & Interfaces. 2015;**7**:9831-9840. DOI: 10.1021/acsami.5b01760

[16] Kar E, Bose N, Dutta B, Banerjee S, Mukherjee N, Mukherjee S. 2D SnO_2 nanosheet/PVDF composite based flexible, self-cleaning piezoelectric energy harvester. Energy Conversion and Management. 2019;**184**:600-608. DOI: 10.1016/j.enconman.2019.01.073

[17] Thakur P, Kool A, Hoque NA, Bagchi B, Khatun F, Biswas P, et al. Superior performances of In situ synthesized ZnO/PVDF thin film based self-poled piezoelectric nanogenerator and self-charged photo-power Bank with high durability. Nano Energy. 2018;**44**:456-467. DOI: 10.1016/j.nanoen.2017.11.065

[18] Saravanakumar B, Soyoon S, Kim SJ. Self-powered pH sensor based on a flexible organic-inorganic hybrid composite nanogenerator. ACS Applied Materials & Interfaces. 2014;**6**:13716-13723. DOI: 10.1021/am5031648

[19] Karan SK, Bera R, Paria S, Das AK, Maiti S, Maitra A, et al. An approach to design highly durable piezoelectric nanogenerator based on self-poled PVDF/AlO-rGO flexible Nanocomposite with high power density and energy conversion efficiency. Advanced Energy Materials. 2016;**6**:1601016. DOI: 10.1002/aenm.201601016

[20] Yaqoob U, Uddin ASMI, Chung G-S. A novel tri-layer flexible piezoelectric nanogenerator based on surface-modified graphene and PVDF-$BaTiO_3$ nanocomposites. Applied Surface Science. 2017;**405**:420-426. DOI: 10.1016/j.apsusc.2017.01.314

[21] Jeong CK, Baek C, Kingon AI, Park KI, Kim SH. Lead-free perovskite nanowire-employed piezopolymer for highly efficient flexible nanocomposite energy harvester. Small. 2018;**14**:e1704022. DOI: 10.1002/smll.201704022

[22] Zhang C, Fan Y, Li H, Li Y, Zhang L, Cao S, et al. Fully rollable lead-free poly(vinylidene fluoride)-niobate-based nanogenerator with ultra-flexible nano-network electrodes. ACS Nano. 2018;**12**:4803-4811. DOI: 10.1021/acsnano.8b01534

[23] Dutta B, Kar E, Bose N, Mukherjee S.NiO@SiO_2/PVDF: A flexible polymer nanocomposite for a high performance human body motion-based energy harvester and tactile e-skin Mechanosensor. ACS Sustainable Chemistry & Engineering. 2018;**6**:10505-10516. DOI: 10.1021/acssuschemeng.8b01851

[24] Maity K, Mandal D. All-organic high-performance piezoelectric nanogenerator with multilayer assembled electrospun nanofiber mats for self-powered multifunctional sensors. ACS Applied Materials & Interfaces. 2018;**10**:18257-18269. DOI: 10.1021/acsami.8b01862

[25] Li J, Chen S, Liu W, Fu R, Tu S, Zhao Y, et al. High performance piezoelectric nanogenerators based on electrospun ZnO Nanorods/poly(vinylidene fluoride) composite membranes. The Journal of Physical Chemistry C. 2019;**123**:11378-11387. DOI: 10.1021/acs.jpcc.8b12410

[26] Cui Z, Hassankiadeh NT, Zhuang Y, Drioli E, Lee YM. Crystalline polymorphism in poly(vinylidenefluoride) membranes. Progress in Polymer Science. 2015;**51**:94-126. DOI: 10.1016/j.progpolymsci.2015.07.007

[27] Li M, Wondergem HJ, Spijkman MJ, Asadi K, Katsouras I, Blom PW, et al. Revisiting the delta-phase of

poly(vinylidene fluoride) for solution-processed ferroelectric thin films. Nature Materials. 2013;**12**: 433-438. DOI: 10.1038/nmat3577

[28] He X, Yao K, Gan BK. Phase transition and properties of a ferroelectric poly(vinylidene fluoride-hexafluoropropylene) copolymer. Journal of Applied Physics. 2005;**97**:084101. DOI: 10.1063/1.1862323

[29] Wegener M, Künstler W, Richter K, Gerhard-Multhaupt R. Ferroelectric polarization in stretched Piezo- and pyroelectric poly(vinylidene fluoride-hexafluoropropylene) copolymer films. Journal of Applied Physics. 2002;**92**:7442-7447. DOI: 10.1063/1.1524313

[30] Jayasuriya AC, Scheinbeim JI. Ferroelectric behavior in solvent cast poly(vinylidene fluoridehexafluoropropylene) copolymer films. Applied Surface Science. 2001;**175-176**:386-390

[31] Kawai H. The piezoelectricity of poly(vinylidene fluoride). Japanese Journal of Applied Physics. 1969;**8**:975-976

[32] Katsouras I, Asadi K, Li M, van Driel TB, Kjaer KS, Zhao D, et al. The negative piezoelectric effect of the ferroelectric polymer poly(vinylidene fluoride). Nature Materials. 2016;**15**:78-84. DOI: 10.1038/nmat4423

[33] Cai X, Lei T, Sun D, Lin L. A critical analysis of the α, β and γ phases in poly(vinylidene fluoride) using FTIR. RSC Advances. 2017;**7**:15382-15389. DOI: 10.1039/c7ra01267e

[34] Jun Li D, Hong S, Gu S, Choi Y, Nakhmanson S, Heinonen O, et al. Polymer piezoelectric energy harvesters for low wind speed. Applied Physics Letters. 2014;**104**:012902. DOI: 10.1063/1.4861187

[35] Kim D, Hong S, Li D, Roh HS, Ahn G, Kim J, et al. A spring-type piezoelectric energy harvester. RSC Advances. 2013;**3**:3194-3198. DOI: 10.1039/c2ra22554a

[36] Ryu J, Kim J, Oh J, Lim S, Sim JY, Jeon JS, et al. Intrinsically stretchable multi-functional Fiber with energy harvesting and strain sensing capability. Nano Energy. 2019;**55**:348-353. DOI: 10.1016/j.nanoen.2018.10.071

[37] Mandal D, Yoon S, Kim KJ. Origin of piezoelectricity in an electrospun poly(vinylidene fluoride-trifluoroethylene) nanofiber web-based nanogenerator and nano-pressure sensor. Macromolecular Rapid Communications. 2011;**32**:831-837. DOI: 10.1002/marc.201100040

[38] Egusa S, Wang Z, Chocat N, Ruff ZM, Stolyarov AM, Shemuly D, et al. Multimaterial piezoelectric fibres. Nature Materials. 2010;**9**:643-648. DOI: 10.1038/nmat2792

[39] Mao Y, Zhao P, McConohy G, Yang H, Tong Y, Wang X. Sponge-like piezoelectric polymer films for scalable and integratable nanogenerators and self-powered electronic systems. Advanced Energy Materials. 2014;**4**:1301624. DOI: 10.1002/aenm.201301624

[40] Madaeni SS, Taheri AH. Effect of casting solution on morphology and performance of PVDF microfiltration membranes. Chemical Engineering & Technology. 2011;**34**:1328-1334. DOI: 10.1002/ceat.201000177

[41] Lee JH, Lee KY, Gupta MK, Kim TY, Lee DY, Oh J, et al. Highly stretchable piezoelectric-pyroelectric hybrid nanogenerator. Advanced Materials. 2014;**26**:765-769. DOI: 10.1002/adma.201303570

[42] Bhavanasi V, Kusuma DY, Lee PS. Polarization orientation,

piezoelectricity, and energy harvesting performance of ferroelectric PVDF-TrFE nanotubes synthesized by nanoconfinement. Advanced Energy Materials. 2014;**4**:1400723. DOI: 10.1002/aenm.201400723

[43] Calahorra Y, Whiter RA, Jing Q, Narayan V, Kar-Narayan S. Localized electromechanical interactions in ferroelectric P(VDF-TrFE) nanowires investigated by scanning probe microscopy. APL Materials. 2016;**4**:116106. DOI: 10.1063/1.4967752

[44] Chen X, Shao J, An N, Li X, Tian H, Xu C, et al. Self-powered flexible pressure sensors with vertically well-aligned piezoelectric nanowire arrays for monitoring vital signs. Journal of Materials Chemistry C. 2015;**3**:11806-11814. DOI: 10.1039/c5tc02173a

[45] Xin Y, Zhu J, Sun H, Xu Y, Liu T, Qian C. A brief review on piezoelectric PVDF nanofibers prepared by electrospinning. Ferroelectrics. 2018;**526**:140-151. DOI: 10.1080/00150193.2018.1456304

[46] Chang C, Limkrailassiri K, Lin L. Continuous near-field electrospinning for large area deposition of orderly nanofiber patterns. Applied Physics Letters. 2008;**93**:123111. DOI: 10.1063/1.2975834

[47] Chang C, Tran VH, Wang J, Fuh Y-K, Lin L. Direct-write piezoelectric polymeric nanogenerator with high energy conversion efficiency. Nano Letters. 2010;**10**:726-731. DOI: 10.1021/nl9040719

[48] Lestoquoy G, Chocat N, Wang Z, Joannopoulos JD, Fink Y. Fabrication and characterization of thermally drawn fiber capacitors. Applied Physics Letters. 2013;**102**:152908. DOI: 10.1063/1.4802783

[49] Lu X, Qu H, Skorobogatiy M. Piezoelectric micro- and nanostructured fibers fabricated from thermoplastic nanocomposites using a fiber drawing technique: Comparative study and potential applications. ACS Nano. 2017;**11**:2103-2114. DOI: 10.1021/acsnano.6b08290

[50] Zhao J, You Z, Shoe A. Embedded piezoelectric energy harvester for wearable sensors. Sensors. 2014;**14**:12497-12510. DOI: 10.3390/s140712497

[51] Jaffe H, Berlincourt DA. Piezoelectric transducer materials. Proceedings of the IEEE. 1965;**53**:1372-1386. DOI: 10.1109/PROC.1965.4253

[52] Takahashi H, Numamoto Y, Tani J, Matsuta K, Qiu J, Tsurekawa S. Lead-free barium titanate ceramics with large piezoelectric constant fabricated by microwave sintering. Japanese Journal of Applied Physics. 2006;**45**:L30-L32. DOI: 10.1143/jjap.45.L30

[53] Park S-E, Shrout TR. Ultrahigh strain and piezoelectric behavior in relaxor based ferroelectric single crystals. Journal of Applied Physics. 1997;**82**:1804-1811. DOI: 10.1063/1.365983

[54] Chen H-J, Han S, Liu C, Luo Z, Shieh H-PD, Hsiao R-S, et al. Investigation of PVDF-TrFE composite with nanofillers for sensitivity improvement. Sensors and Actuators A: Physical. 2016;**245**:135-139. DOI: 10.1016/j.sna.2016.04.056

[55] Paik H, Choi YY, Hong S, No K. Effect of Ag nanoparticle concentration on the electrical and ferroelectric properties of Ag/P(VDF-TrFE) composite films. Scientific Reports. 2015;**5**:13209. DOI: 10.1038/srep13209

[56] Xu S, Poirier G, Yao N. Fabrication and piezoelectric property of PMN-PT nanofibers. Nano Energy. 2012;**1**:602-607. DOI: 10.1016/j.nanoen.2012.03.011

[57] Chan HLW, Chen Y, Choy CL. A poling study of PZT/P(VDF-TrFE) copolymer 0-3 composites. Integrated Ferroelectrics. 2006;**9**:207-214. DOI: 10.1080/10584589508012925

[58] Kim HS, Lee DW, Kim DH, Kong DS, Choi J, Lee M, et al. Dominant role of Young's modulus for electric power generation in PVDF-$BaTiO_3$ composite-based piezoelectric nanogenerator. Nanomaterials (Basel). 2018;**8**:777. DOI: 10.3390/nano8100777

[59] Kobayashi Y, Tanase T, Tabata T, Miwa T, Konno M. Fabrication and dielectric properties of the $BaTiO_3$–polymer nano-composite thin films. Journal of the European Ceramic Society. 2008;**28**:117-122. DOI: 10.1016/j.jeurceramsoc.2007.05.007

[60] Kim P, Doss NM, Tillotson JP, Hotchkiss PJ, Pan M-J, Marder SR, et al. High energy density nanocomposites based on surface-modified $BaTiO_3$ and a ferroelectric polymer. ACS Nano. 2009;**3**:2581-2592. DOI: 10.1021/nn9006412

[61] Cha S, Kim SM, Kim H, Ku J, Sohn JI, Park YJ, et al. Porous PVDF as effective sonic wave driven nanogenerators. Nano Letters. 2011;**11**:5142-5147. DOI: 10.1021/nl202208n

[62] Lang C, Fang J, Shao H, Ding X, Lin T. High-sensitivity acoustic sensors from nanofibre webs. Nature Communications. 2016;**7**:11108. DOI: 10.1038/ncomms11108

[63] Sun B, Li X, Zhao R, Ji H, Qiu J, Zhang N, et al. Electrospun poly(vinylidene fluoride)-zinc oxide hierarchical composite Fiber membrane as piezoelectric acoustoelectric nanogenerator. Journal of Materials Science. 2018;**54**:2754-2762. DOI: 10.1007/s10853-018-2985-x

[64] Cuadras A, Gasulla M, Ferrari V. Thermal energy harvesting through pyroelectricity. Sensors and Actuators A: Physical. 2010;**158**:132-139. DOI: 10.1016/j.sna.2009.12.018

[65] Vuorinen T, Zakrzewski M, Rajala S, Lupo D, Vanhala J, Palovuori K, et al. Printable, transparent, and flexible touch panels working in sunlight and moist environments. Advanced Functional Materials. 2014;**24**:6340-6347. DOI: 10.1002/adfm.201401140

[66] Talemi P, Delaigue M, Murphy P, Fabretto M. Flexible polymer-on-polymer architecture for piezo/pyroelectric energy harvesting. ACS Applied Materials & Interfaces. 2015;**7**:8465-8471. DOI: 10.1021/am5089082

[67] Zabek D, Taylor J, Boulbar EL, Bowen CR. Micropatterning of flexible and free standing polyvinylidene difluoride (PVDF) films for enhanced pyroelectric energy transformation. Advanced Energy Materials. 2015;**5**:1401891. DOI: 10.1002/aenm.201401891

[68] Zabek D, Seunarine K, Spacie C, Bowen C. Graphene ink laminate structures on poly(vinylidene difluoride) (PVDF) for pyroelectric thermal energy harvesting and waste heat recovery. ACS Applied Materials & Interfaces. 2017;**9**:9161-9167. DOI: 10.1021/acsami.6b16477

[69] Bell AJ, Deubzer O. Lead-free piezoelectrics—The environmental and regulatory issues. MRS Bulletin. 2018;**43**:581-587. DOI: 10.1557/mrs.2018.154

[70] Setter N, Damjanovic D, Eng L, Fox G, Gevorgian S, Hong S, et al. Ferroelectric thin films: Review of materials, properties, and applications. Journal of Applied Physics. 2006;**100**:051606. DOI: 10.1063/1.2336999

[71] Kim J, Hong S, Bühlmann S, Kim Y, Park M, Kim YK. et al. Effect

of deposition temperature of TiO_2 on the piezoelectric property of $PbTiO_3$ film grown by PbO gas phase reaction sputtering. Journal of Applied Physics. 2010;**107**:104112. DOI: 10.1063/1.3406148

[72] Panda PK, Sahoo B. PZT to lead free piezo ceramics: A review. Ferroelectrics. 2015;**474**:128-143. DOI: 10.1080/00150193.2015.997146

[73] Bayer IS, Tiwari MK, Megaridis CM. Biocompatible poly(vinylidene fluoride)/ cyanoacrylate composite coatings with tunable hydrophobicity and bonding strength. Applied Physics Letters. 2008;**93**:173902. DOI: 10.1063/1.3009292

[74] Guo HF, Li ZS, Dong SW, Chen WJ, Deng L, Wang YF, et al. PVDF electrospun scaffolds for wound healing applications. Colloids and Surfaces B: Biointerfaces. 2012;**96**:29-36. DOI: 10.1016/j.colsurfb.2012.03.014

[75] Yu Y, Sun H, Orbay H, Chen F, England CG, Cai W, et al. Biocompatibility and in vivo operation of implantable mesoporous PVDF-based nanogenerators. Nano Energy. 2016;**27**:275-281. DOI: 10.1016/j.nanoen.2016.07.015

[76] Li J, Kang L, Yu Y, Long Y, Jeffery JJ, Cai W, et al. Study of Long-term biocompatibility and bio-safety of implantable nanogenerators. Nano Energy. 2018;**51**:728-735. DOI: 10.1016/j.nanoen.2018.07.008